CHAPTER - II

CHAPTER II

PREPARATION OF FERRITES AND CHARACTERIZATION BY X-RAY DIFFRACTION.

INTRODUCTION

2.1 METHODS OF PREPARATION

2.1.1 CERAMIC METHOD

2.1.2 DECOMPOSITION METHOD

2.1.3 HYDROXIDE PRECIPITATION METHOD

2.1.4 OXALATE PRECIPITATION METHOD

2.2 PREPARATION OF FERRITE SAMPLES

2.3 X RAY DIFFRACTION

2.4 EXPERIMENTAL

2.5 INDEXING OF XRD PATTERNS AND CALCULATION OF LATTICE PARAMETERS

2.6 RESULTS AND DISCUSSION

REFERENCES

INTRODUCTION

The properties of ferrites are the results of their internal structure. They are very much sensitive to the conditions of preparation,chemical composition and are highly influenced by their crystal structure and cation distribution. Moreover, the microstructural factors like porosity, grain size,grain distribution and density also affect their properties considerably. Thus in order to establish a clear relationship between the properties and the above factors, much attention needs to be given towards their methods of preparation.

In this chapter a brief review of methods of ferrites preparation is given. The ceramic method used in the present case has been emphasized. The method of characterizing ferrites by X-ray diffraction is discussed. The results are discussed at the end.

2.1 METHODS OF PREPARATION

These ferrites are oxide-magnetic ceramics and so cannot be easily moulded in the desired shape by melting as in the case of metals. Though there are several methods of ferrite preparation in use,the ceramic technique discussed below seems to be suitable from this point of view. The ferrite fabrication technique generally involves the following steps (Fig. 2.1)

1. Preparation of ferrites containing required proportions of metal ions.

2. Compacting the ferrite powder to its desired shape

   and

3. Sintering the compact at high temperature to get the final product with adequate grain size and density.

The following methods of ferrite preparation are currently in use.

1. Oxide method or ceramic method.

2. Decomposition method.

3. Hydroxide precipitation method and

4. Oxalate precipitation method.

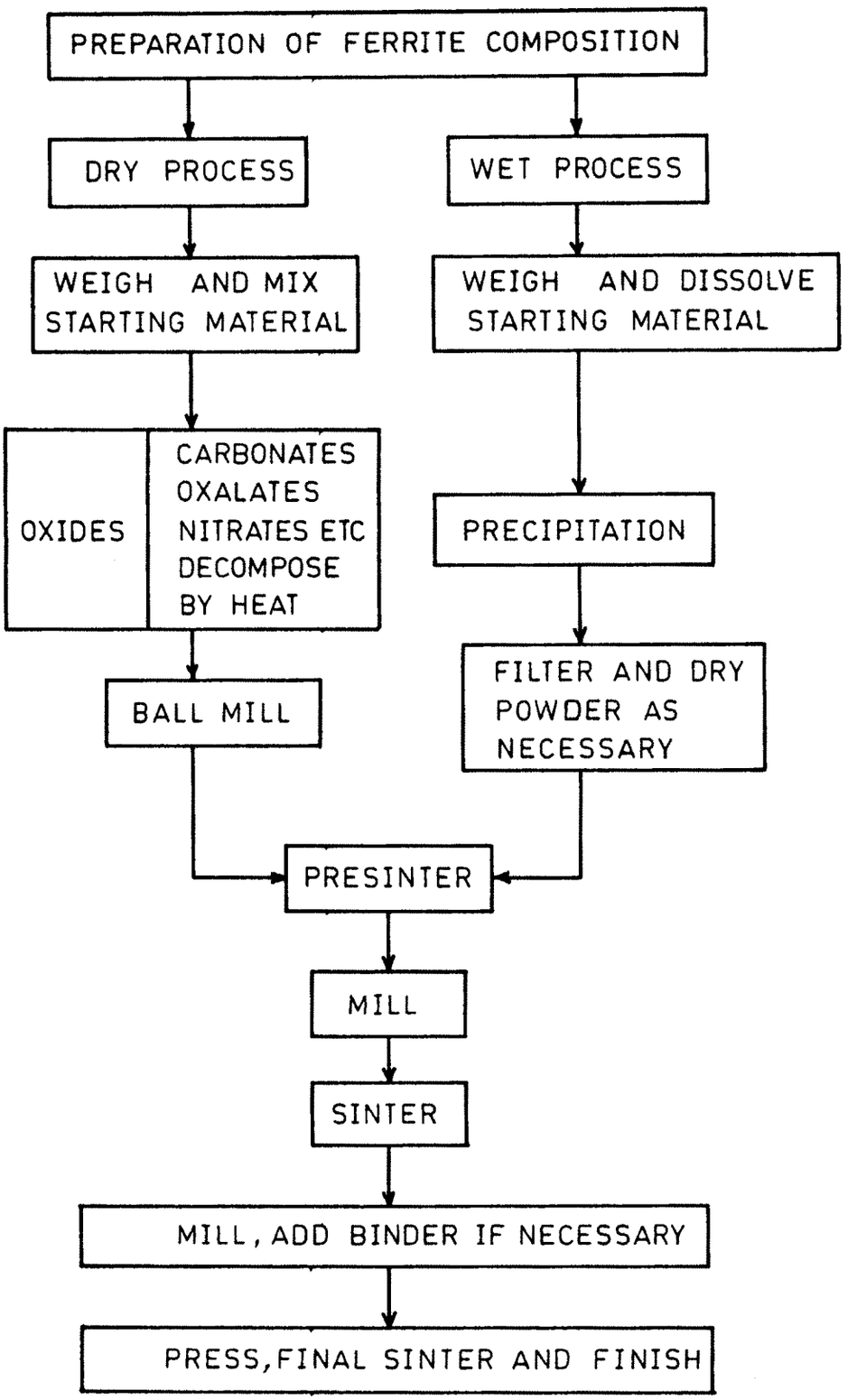

FIG.2.1 FLOW CHART OF STAGES IN THE FERRITE PREPARATION.

2.1.1. CERAMIC METHOD

The method of ferrite preparation by this method is essentially a solid state reaction between the component oxides to form a resultant ferrite. In this method high purity divalent metal oxides are physically intimately mixed with iron oxide using the ball mill. The mixture is presintered at a suitable temperature for the desired duration. It is furnace cooled,mechanically powdered and sieved to avoid the undesired large sized particles. The powder is pressed in the die to obtain the required shape and subjected to final sintering at high temperatures. The method is comparatively simpler and gives good results. Also, the method is probably the easiest to use with little chemical knowledge.

2.1.2 DECOMPOSITION METHOD

Instead of using oxides as starting materials, one may commence with salts such as carbonates, nitrates and oxalates, which may be mixed (milled)in the requisite

proportions. The salts are then preheated, usually in air,to produce the oxides by thermal decomposition. In all other details this method is similar to the oxide method.

2.1.3 HYDROXIDE PRECIPITATION METHOD

The hydroxides are precipitated simultaneously from a solution, so that the precipitate contains the required metal ions in the correct proportions. Economos (1) established this method for ferrite preparation. Recently, Robbins(2) prepared manganese zinc ferrite by chemical co-precipitation with hydroxide and carbonate. The hydroxide precipitation method is also applied for the preparation of yttrium iron garnet by Wolf et al (3). The qualitative understanding of chemical process involved is essential, because the simultaneous precipitation of the hydroxides must be complete. Sato et al (4.5) prepared ultrafine spinel ferrites by this method.

2.1.4 OXALATE PRECIPITATION

Precipitation of the metallic oxalates is preferable for two reasons. Firstly, precipitation can be carried out using ammonium oxalate which does not leave any residue after ignition. Secondly, most of the metal oxalates are very similar in crystal structure; the precipitation tends, therefore to produce mixed crystals which contain the metallic cations in the proportions in which they were present in the solution. Thus the mixing in the correct ratios can be achieved on a molecular scale. Mixed crystals do not form uniformly if precipitation occurs at widely differing rates. Careful calcining of the precipitate at a temperature near to 600° C in the case of $MgFe_2O_4$, yielded a ferrite with an average particle size less than 1 micron.

2.2 PREPARATION OF FERRITE SAMPLES

Of all the methods of ferrite preparation the ceramic method is the simplest and straightforward. As a result the same method has been used for the large scale industrial manufacturing of ferrites.

In the present case Magnesium oxide (MgO),Zinc oxide(ZnO) and Iron oxide (Fe_2O_3) were used as the starting chemicals. All of them were of high quality and purity.

The raw materials were weighted accurately by using a semimicrobalance to the required molar proportion dictated by the chemical formula of the samples viz.$Mg_xZn_{(1-x)}Fe_2O_4$. The ferrites with x=0.0, 0.2, 0.4, 0.6, 0.8 and 1.0 were prepared.

The compositional weights of powders were mixed thoroughly in the acetone medium using the agate mortar. The dry powders of samples were presintered at 800° C for 15 hours by keeping them separately in clean dry platinum crucibles. For the purpose of presintering and final sintering a globar furnace fabricated in the department was used. The samples were furnace cooled at the rate of 80° C / hr. The presintered powders were subjected to mechanical blending in acetone medium for six hours. The powders were dried again and sieved so as to eliminate any large sized particles.

In order to prepare the sample pellets, a small quantity of the presintered powder was ground in 50 cc of acetone with one or two drops of polyvinyl acetate. The later works as a binder. This powder was then introduced in the bore of a steel die of 1 cm diameter. A pressure of about 10 tons/inch^2 was applied to the die by using a commercial hydraulic press. The pellets were slowly removed from the die after two to three minutes. Two sets of pellets were made so as to enable them to be final sintered at two different sintering times.

Final sintering of the pellets was carried out at 1100° C for 15 hr. and 30 hr. respectively by keeping them on platinum sheets. The pellets were furnace cooled,removed from the furnace and polished for use in experiments.

2.3 X RAY DIFFRACTION

X ray diffraction technique is on of the well established techniques for the study of crystal structure of materials. It has been used both for the confirmation of the spinel structure and to determine the lattice parameters as far as ferrites are concerned.

The simplest explanation of the observed diffraction maxima when X-ray radiation passes through the crystal was first given by Bragg (6). The diffraction maxima occur when Bragg's law, viz. 2d Sin = n is satisfied. Different methods of crystal structure evaluation are available depending upon whether the O (diffraction angle) or the (wavelength of X-rays) is varied. For all powder diffraction work the wavelength of the X-rays is kept constant (i.e. monochromatic X-rays used) and the sample is rotated in order to vary the Bragg angle. The method is popularly known as the powder method and used in the present case.

The powder method was developed by Debye and Scherrer (7), and independently by Hull (8). In this method a small quantity of smoothly ground powder sample is coated on a fine glass capillary with the help of a glue. The specimen is mounted on the movable mount provided at the centre of Debye - scherrer camera after proper alignment. Since the fine grains of the powder sample are randomly oriented, the reciprocal lattice vectors of all the crystallites are pointed in all possible directions. The incident monochromatic X-ray radiation finds some crystal planes which satisfy the Bragg diffraction condition to produce the diffraction maxima. Since the diffracted X-rays from a particular set of planes lie along the surface of a cone with apex angle 2θ, when they intercept the film, they produce concentric ring. The cones coming from different set of planes similarly produce different concentric rings on the film. To ensure that all possible sets of planes face the incident monochromatic beam the sample is rotated with the help of an electric motor. In an XRD machine a counter is used instead of a film and a direct graphical record of intensities of

diffracted maxima as a function of 2θ is obtained.

2.4 EXPERIMENTAL

X-ray diffraction patterns of the samples in the system $Mg_xZn_{(1-x)}Fe_2O_4$ with x = 0.0, 0.2, 0.4, 0.6, 0.8 and 1.0 were taken by using filtered Fe-kα radiation. The machine was operated at 30,000 Volts potential and filament current was kept at 15 mA. The diffractometer facility was availed from the Mineralogical Institute,University of Mysore,Mysore. The range of 2θ angles between which the diffractograms were taken was 10° to 85°. The rate of angular displacement of the counter was adjusted to 1° /min.

2.5 INDEXING OF XRD PATTERNS AND CALCULATION OF LATTICE PARAMETERS

As mentioned earlier, the diffraction maxima occur when the Bragg's law is satisfied. viz.

$$2d \sin \theta = n\lambda \quad \text{----------2.1}$$

For a cubic system the interplaner distance d is given by

$$d = a/[h^2+k^2+l^2]^{1/2} \quad \text{----------2.2}$$

where a is the lattice parameter and hkl are Miller indices of the reflecting plane. Eliminating d from eqns. 2.1 and 2.2, we get

$$a = \lambda/2\sin\theta\ (h^2+k^2+l^2)^{1/2} \quad \text{----------2.3}$$

Lattice parameters are calculated by using the relation 2.3.

In the XRD pattern of a spinel ferrite the (311) reflection is prominent and easily identifiable from the diffraction pattern. The corresponding value of 2θ is noted and θ, Sinθ, $\sin^2\theta$ are determined. Substituting the values in eqn.2.3 the lattice parameter is calculated.

e.g.consider the case of $MgFe_2O_4$. The (311) reflection occurs at 2θ value equal to 45° . ... Fig. 2.6

$$\theta = 22.5^\circ$$
$$\sin\theta = 0.3827$$

Since λ = 1.936 A° for Fe-Kα radiation,eqn.2.3 gives

$$a = 8.378\ A^\circ.$$

Knowing the value of a,it is possible to index other reflections adopting the following procedure .

Consider a peak with

$$2\theta = 23.08$$
$$\theta = 11.54$$
$$\sin\theta = 0.2001$$
$$\sin^2\theta = 0.4004$$

from 2.3

$$(h^2+k^2+l^2) = [4a^2\sin^2\theta]/\lambda^2 \text{ ----------2.4}$$

Substituting the values of a, $\sin^2\theta$ and λ in the proper form, equation 2.4 gives

$$h^2+k^2+l^2 = 3.1013$$

which is approximately equal to 3. The corresponding reflection can be readily indexed as (111). All other reflections were indexed similarly. Due care was taken to evaluate accurate lattice parameters using the standard refinement techniques.

2.6 RESULTS AND DISCUSSION.

The diffraction patterns of all the samples studied in the present case are shown in figs. 2.2 to 2.7. The data regarding the diffracting planes, observed and calculated d values, lattice parameters and porosity etc., is presented in tables 2.1, 2.2, 2.3, 2.4, 2.5, 2.6, 2.7, 2.8.

As stated earlier the ferrites possess the structure of mineral spinel ($MgAl_2O_4$) that crystallizes in the cubic form with space group $Fd3m-0^7_h$. The diffraction maxima have been indexed in the light of the crystal structure data of natural spinel. The refections observed are (111), (220), (311), (400), (420), (422), (333). They are in conformity with the allowed reflections in the spinel structure. Also the observed and calculated d values are in well agreement with each other. Since there is no presence of any other extra reflection, it can be stated that the ferrites with spinel structure have been formed during the preparation stage.

The calculated values of lattice parameters for our samples are presented in tables 2.1 to 2.6 along with their compositions. A systematic variation of lattice parameter a, as a function of Zn content is shown in fig.2.8. It can be observed that as the amount of Zinc in ferrite sample increases,the lattice parameter also increases. It is minimum for $MgFe_2O_4$ and maximum for

$ZnFe_2O_4$. The reported values of lattice parameters are in close agreement with the values reported earlier (9,10). It would be worthwhile to note here that there are considerable deviations in the lattice constants of Magnesium and Zinc ferrites as reported in the literature (9,10). For Magnesium ferrite it varies from 8.375 A° to 8.36 A° (11,12) and for Zinc ferrite from 8.44 A° to 8.416 A° (13,14) respectively. Linear variation of lattice parameter with the content of Zinc shows that the famous Vegard's law is obeyed by our samples. Since the ionic radii of Mg and Zn are 0.75 A° and 0.83 A° respectively, it is expected that as the content of Zinc in the sample increases the lattice parameter should increase. The same trend has been observed here.

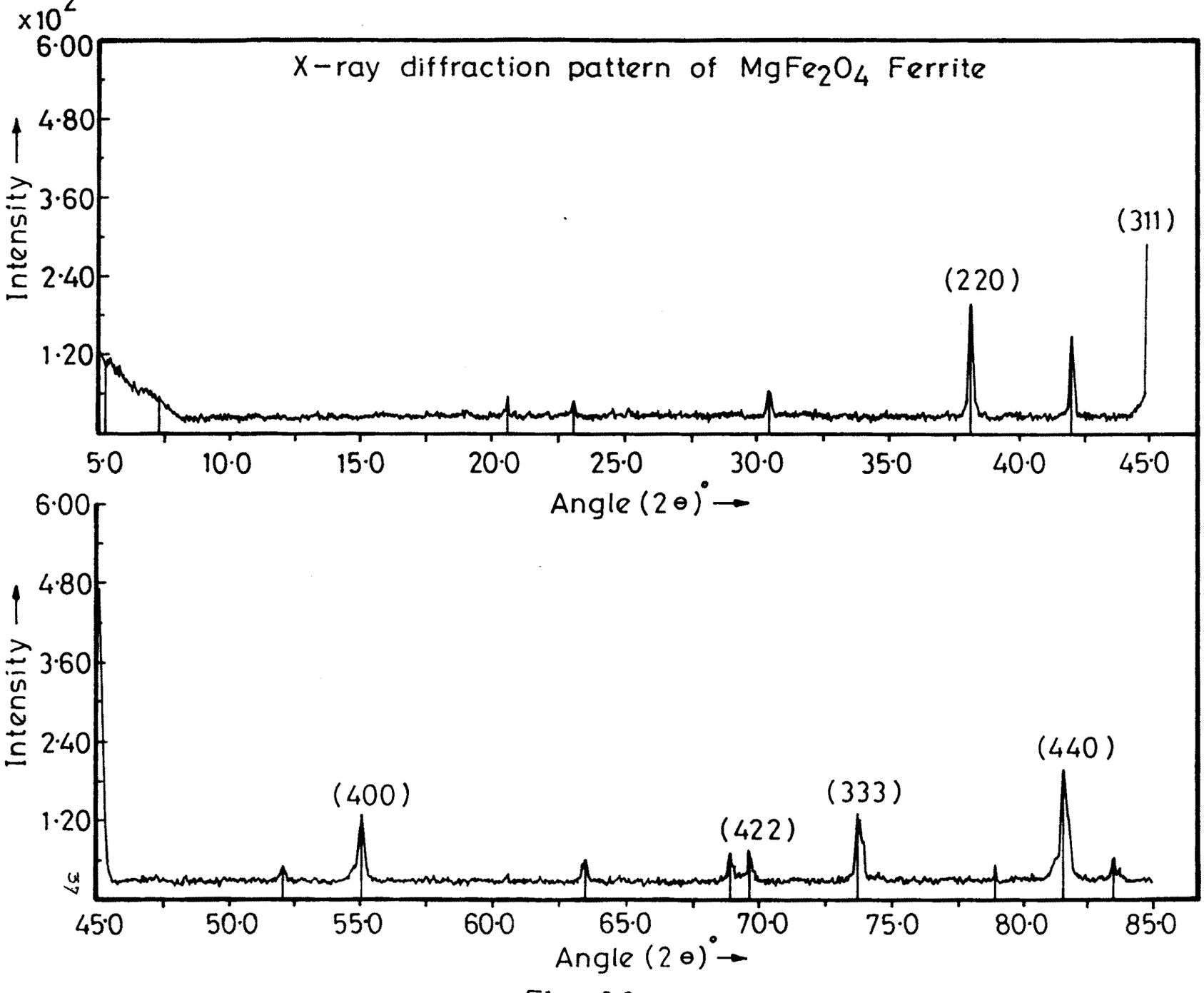
X-ray diffraction pattern of $MgFe_2O_4$ Ferrite
x10²
6·00
4·80
3·60
2·40
1·20
Intensity
(220)
(311)
5·0
10·0
15·0
20·0
25·0
30·0
35·0
40·0
45·0
Angle (2θ)°
(400)
(422)
(333)
(440)
45·0
50·0
55·0
60·0
65·0
70·0
75·0
80·0
85·0

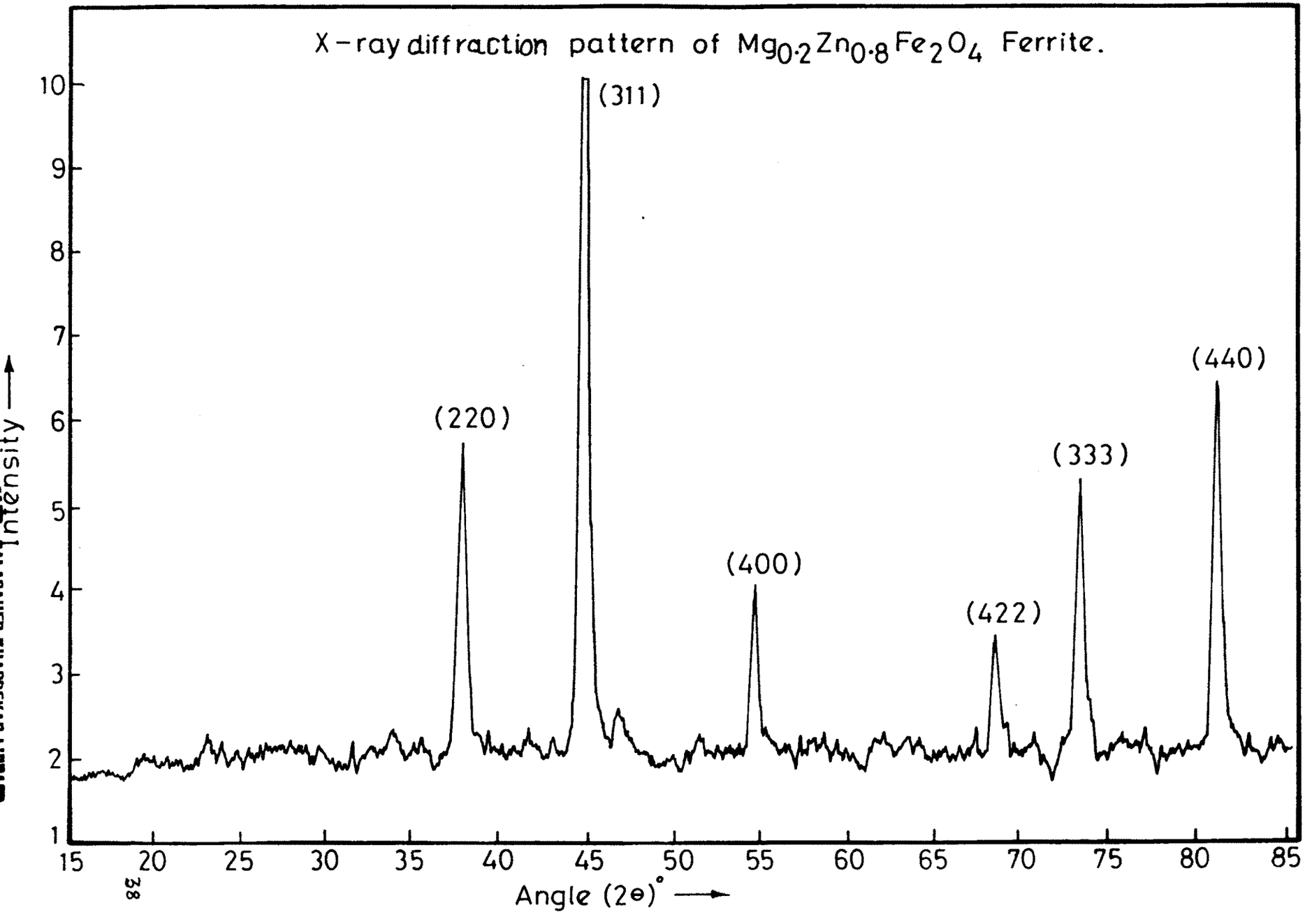

Fig.– 2.3

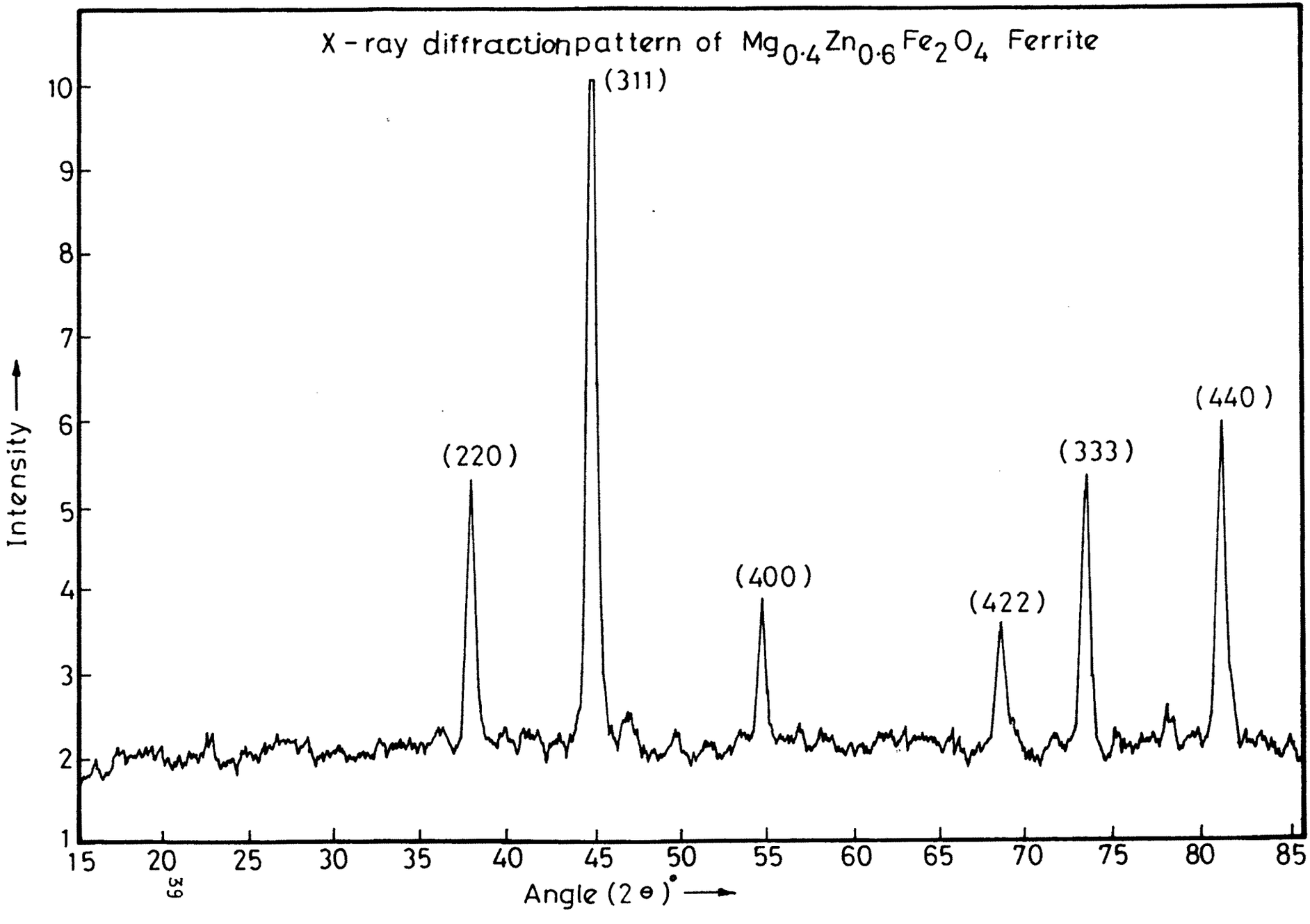
X - ray diffractionpattern of $Mg_{0.4}Zn_{0.6}Fe_2O_4$ Ferrite
(220)
(311)
(400)
(422)
(333)
(440)
Intensity
Angle (2θ)°
1
2
3
4
5
6
7
8
9
10
15
20
25
30
35
40
45
50
55
60
65
70
75
80
85

Fig.– 2.4

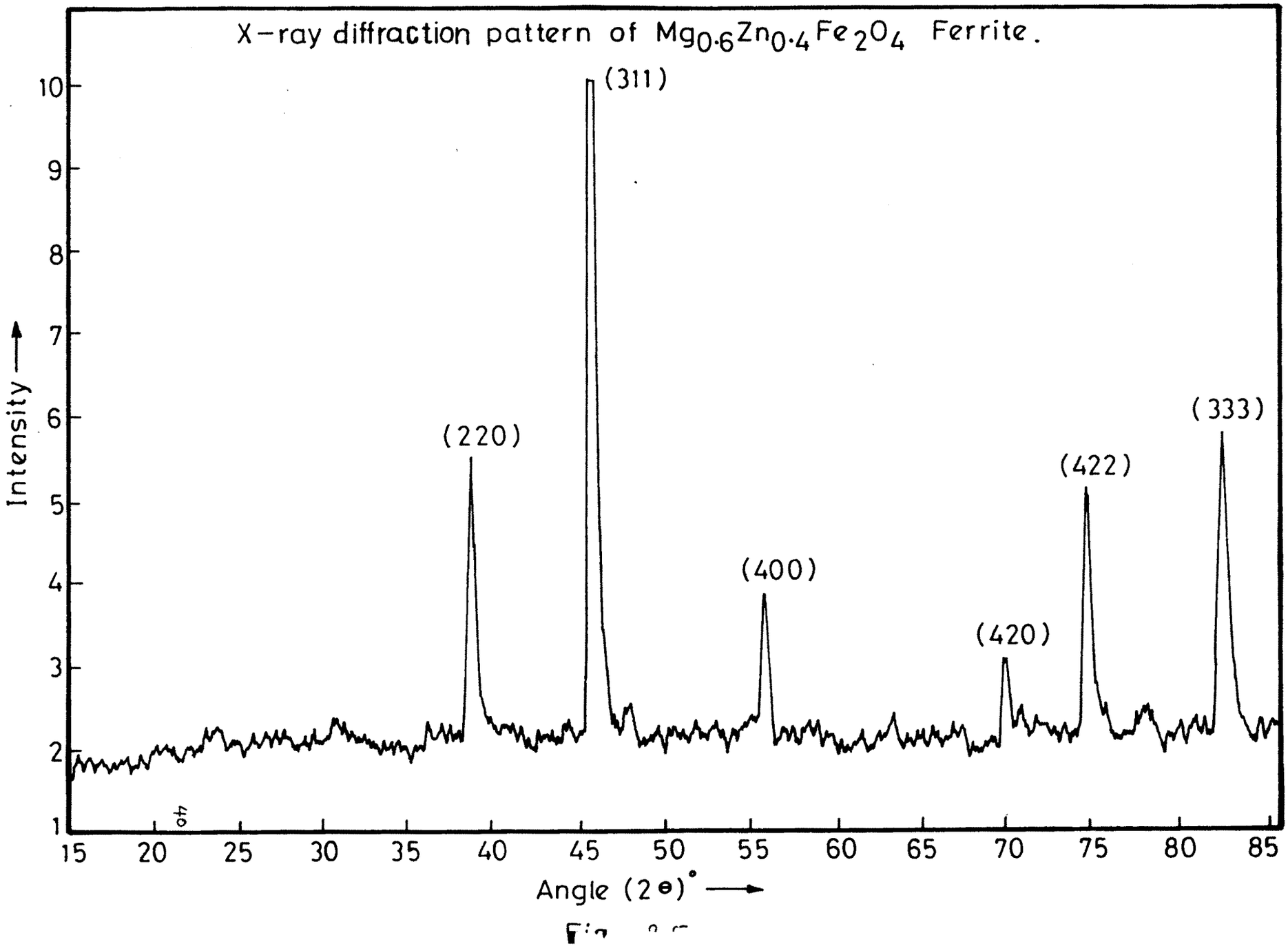
X-ray diffraction pattern of $Mg_{0.6}Zn_{0.4}Fe_2O_4$ Ferrite.
(311)
(220)
(400)
(420)
(422)
(333)
Intensity
Angle (2θ)°
10
9
8
7
6
5
4
3
2
1
15
20
25
30
35
40
45
50
55
60
65
70
75
80
85

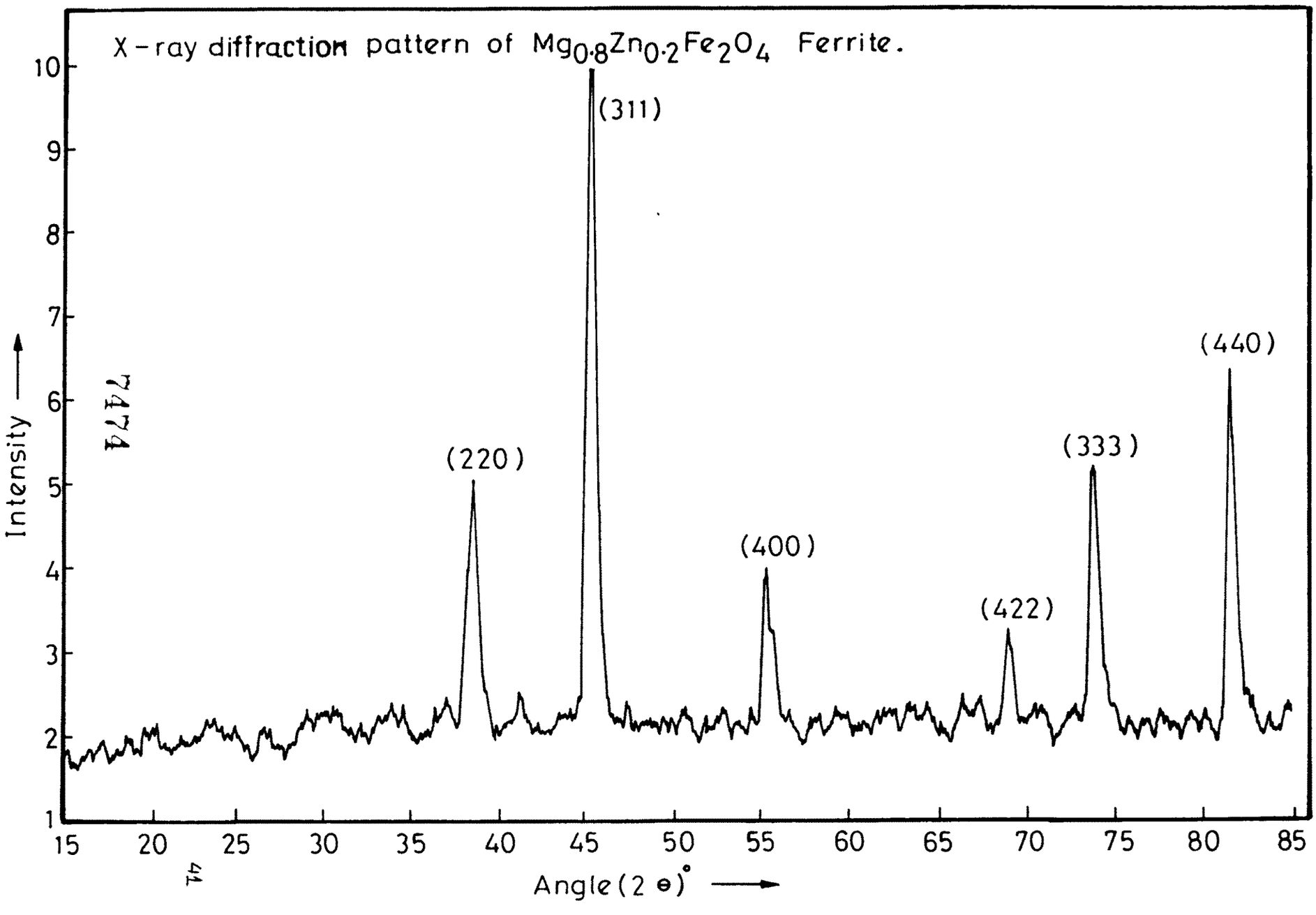
X-ray diffraction pattern of $Mg_{0.8}Zn_{0.2}Fe_2O_4$ Ferrite.
(220)
(311)
(400)
(422)
(333)
(440)
Intensity
Angle (2 θ)°
10
9
8
7
6
5
4
3
2
1
15
20
25
30
35
40
45
50
55
60
65
70
75
80
85

Fig.—2.6

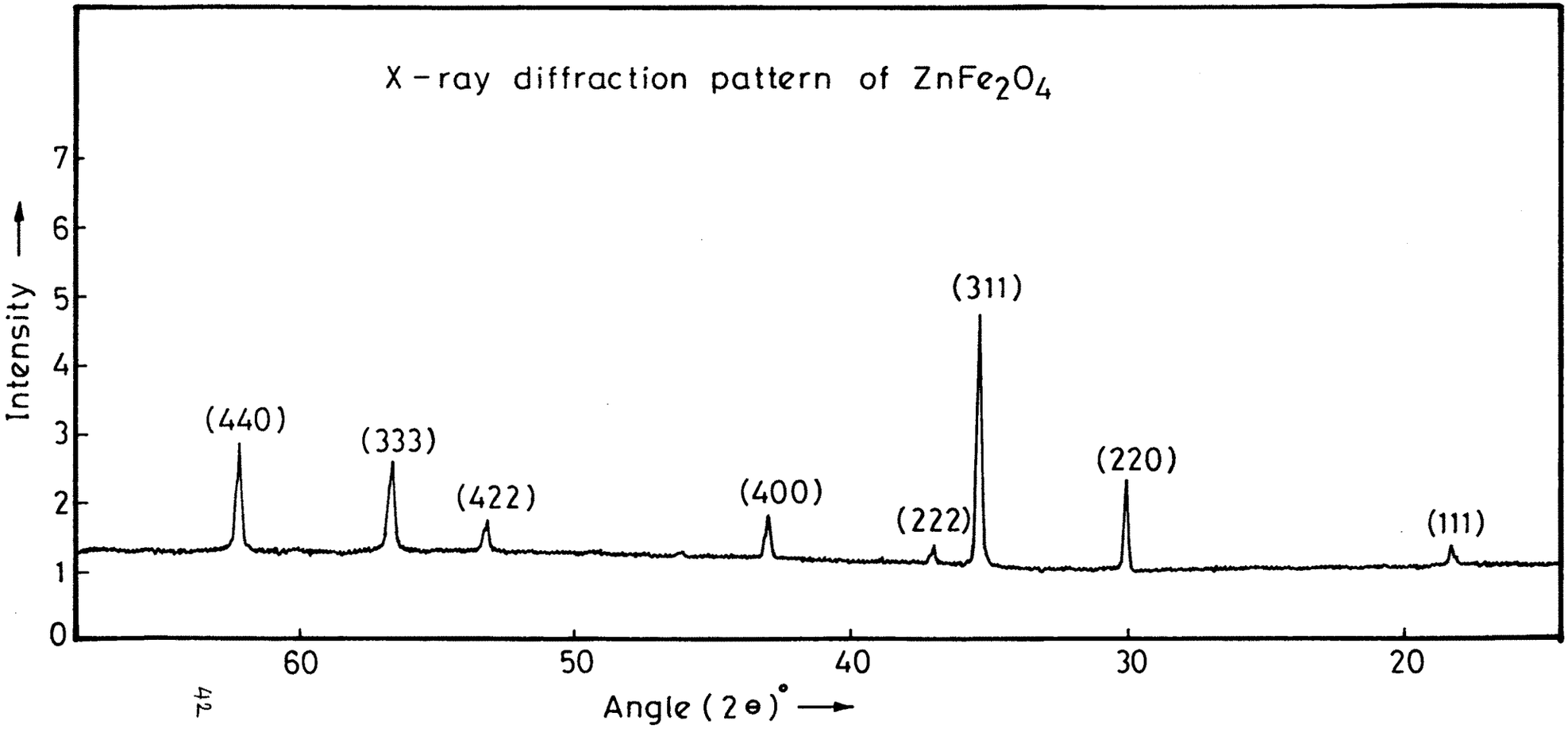
X-ray diffraction pattern of $ZnFe_2O_4$
Intensity
0
1
2
3
4
5
6
7
(440)
(333)
(422)
(400)
(222)
(311)
(220)
(111)
60
50
40
30
20
Angle (2θ)°

Fig. 2.7

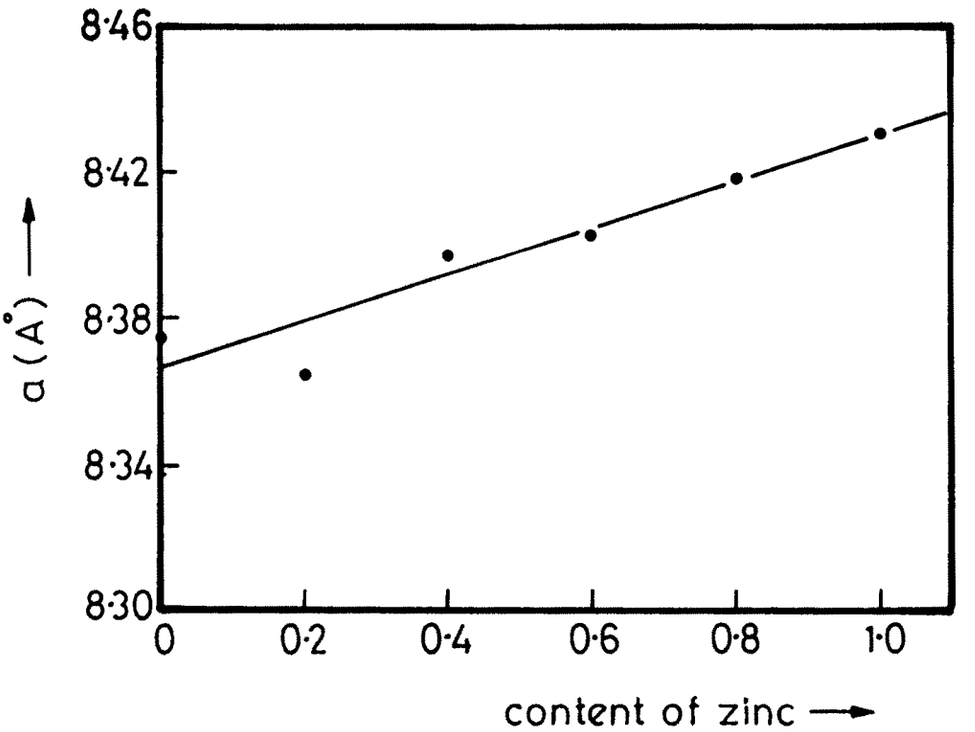

Fig.—2·8

TABLE - 2.1

Sample : $ZnFe_2O_4$
Structure : Cubic

a = 8.431 A°, = 1.5418 A°
Sample sintered at 1100 °C for 30 hours

2θ (°)	θ (°)	Sin θ	Planes (hkl)	Interplaner distance, d, A° (Observed)	Interplaner distance d, A° (Calculated)
30.10	15.05	0.2596	220	2.975	2.981
35.35	17.68	0.3034	311	2.541	2.542
37.00	18.50	0.3173	222	2.430	2.434
43.08	21.44	0.3657	400	2.108	2.108
53.15	26.58	0.4422	422	1.724	1.721
56.65	28.33	0.4744	333	1.625	1.623
62.15	31.08	0.5160	440	1.494	1.490

TABLE -2.2

Sample : $Mg_{0.2}Zn_{0.8}Fe_2O_4$ a = 8.419 A°, = 1.93604 A°
Structure : Cubic Sample sintered at 1100°C for 30 hours

2θ (°)	θ (°)	Sin θ	Planes (hkl)	Interplaner distance, d, A° (Observed)	Interplaner distance d, A° (Calculated)
23.15	11.570	0.20056	111	4.8264	4.8269
38.00	19.000	0.32557	220	2.9732	2.9755
44.85	22.425	0.38150	311	2.5370	2.5370
54.75	27.375	0.45980	400	2.1050	2.1050
68.68	34.340	0.56410	422	1.7160	1.7160
73.42	36.710	0.05977	333	1.6190	1.6190
81.22	40.610	0.65091	440	1.4871	1.4872

TABLE -2.3

Sample : $Mg_{0.4}Zn_{0.6}Fe_2O_4$ a = 8.403 A°, = 1.936 A°
Structure : Cubic Sample sintered at 1100°C for 30 hours

2θ (°)	θ (°)	Sin θ	Planes (hkl)	Interplaner distance, d, A° (Observed)	Interplaner distance d, A° (Calculated)
23.00	11.500	0.19936	111	4.8419	4.8550
38.10	19.050	0.32639	220	2.9658	2.9658
44.90	22.450	0.38187	311	2.8028	2.8027
54.60	34.300	0.56350	422	1.7178	1.7178
73.70	36.850	0.59970	333	1.6141	1.6140
68.60	34.300	0.56350	422	1.7170	1.7180
81.25	40.625	0.65110	440	1.4867	1.4867

TABLE – 2.4

Sample : $Mg_{0.6}Zn_{0.4}Fe_2O_4$ a = 8.399 A°, = 1.936 A°
Structure : Cubic Sample sintered at 1100°C for 30 hours

2θ (°)	θ (°)	Sin θ	Planes (hkl)	Interplaner distance, d, A° (Observed)	Interplaner distance d, A° (Calculated)
23.31	11.650	0.20190	111	4.7940	4.7950
38.31	19.155	0.32281	220	2.9500	2.9500
45.22	22.610	0.38450	311	2.5180	2.5180
55.14	27.570	0.46280	400	2.0920	2.0910
69.10	34.550	0.51650	420	1.8743	1.8740
73.75	36.875	0.54740	422	1.7685	1.7680
81.90	40.950	0.59980	333	1.6140	1.6120

TABLE - 2.5

Sample : $Mg_{0.8}Zn_{0.2}Fe_2O_4$ a = 8.362 A°, = 1.936 A°
Structure : Cubic Sample sintered at 1100°C for 30 hours

2θ (°)	θ (°)	Sin θ	Planes (hkl)	Interplaner distance, d, A° (Observed)	Interplaner distance d, A° (Calculated)
38.50	19.250	0.3297	220	2.9361	2.9460
45.33	22.665	0.3853	311	2.5121	2.5121
55.47	27.735	0.4654	400	2.0800	2.0830
69.10	34.550	0.5671	422	1.7070	1.7010
74.00	37.000	0.6018	333	1.6090	1.6090
81.78	40.890	0.6546	440	1.4790	1.4790

TABLE - 2.6

Sample : $MgFe_2O_4$
Structure : Cubic

a = 8.378 A°, = 1.936 A°
Sample sintered at 1100°C
for 30 hours

2θ (°)	θ (°)	Sin θ	Planes (hkl)	Interplaner distance, d, A° (Observed)	Interplaner distance d, A° (Calculated)
23.08	11.54	0.2001	111	4.8390	4.8610
38.14	19.07	0.3267	220	2.9630	2.9630
45.00	22.50	0.3827	311	2.5290	2.9298
55.07	27.54	0.4620	400	2.0960	2.0950
69.68	34.84	0.5712	422	1.6950	1.6950
73.75	36.87	0.6002	333	1.6129	1.6128
81.56	40.78	0.6532	440	1.4820	1.4810

TABLE - 2.7

PHYSICAL AND X RAY DENSITY DATA FOR SAMPLES SINTERED AT 1100°C FOR 15 HOURS

Sr. No.	Chemical Formula	Molecular Weight	Lattice Constant a, (A°)	Porosity	Physical Density da(g/cm^3)	X-ray Density dx(g/cm^3)
1	$MgFe_2O_4$	199.228	8.378	0.31970	3.0619	4.5007
2	$Mg_{0.8}Zn_{0.2}Fe_2O_4$	207.440	8.362	0.35920	3.0270	4.7131
3	$Mg_{0.6}Zn_{0.4}Fe_2O_4$	215.651	8.399	0.35610	3.1132	4.8352
4	$Mg_{0.4}Zn_{0.6}Fe_2O_4$	223.863	8.403	0.36490	3.1838	5.0122
5	$Mg_{0.2}Zn_{0.8}Fe_2O_4$	232.228	8.419	0.35160	3.3520	5.1690
6	$ZnFe_2O_4$	240.290	8.431	0.28220	3.8230	5.3260

TABLE - 2.8

PHYSICAL AND X RAY DENSITY DATA FOR SAMPLES SINTERED AT 1100°C FOR 30 HOURS

Sr. No.	Chemical Formula	Molecular Weight	Lattice Constant a, (A°)	Porosity	Physical Density da(g/cm^3)	X-ray Density dx(g/cm^3)
1	$MgFe_2O_4$	199.228	8.378	0.27780	3.2508	4.5007
2	$Mg_{0.8}Zn_{0.2}Fe_2O_4$	207.440	8.362	0.34990	3.0639	4.7131
3	$Mg_{0.6}Zn_{0.4}Fe_2O_4$	215.651	8.399	0.39070	2.9460	4.8352
4	$Mg_{0.4}Zn_{0.6}Fe_2O_4$	223.863	8.403	0.34760	3.2698	5.0122
5	$Mg_{0.2}Zn_{0.8}Fe_2O_4$	232.228	8.419	0.31714	3.4269	5.1690
6	$ZnFe_2O_4$	240.290	8.431	0.25291	3.9780	5.3260

The data regarding the band lengths R_A and R_B is contained in table 2.9 and the systematic variation of the bond lengths as a function of Zinc context is presented in figs. 2.9 and 2.10. The average bond lengths have been calculated by using the formulae.

$$R_A = a\,3^{1/2}\,(1/8+\delta) \quad \text{---------- 2.5}$$

$$R_B = a\,[1/16 - \delta/2 + 3\delta 2]^{1/2} \quad \text{------- 2.6}$$

and $$\delta = u - 0.375 \quad \text{---------- 2.7}$$

Here R_A and R_B stand for average shortest distances between A site cations and oxygen ions and the B site cations and oxygen ions, respectively; δ is the deviation from oxygen parameter. The data for u values for these ferrites is reported by Standley (15). It can be seen from fig. 2.9 that the value of R_A goes on increasing as the content of Zinc in the ferrite samples increases, R_A being minimum for Magnesium ferrite and maximum for Zinc ferrite. Such a rise in R_A value can be associated with the corresponding rise in the lattice parameters of the sample. Since Zinc ferrite is the normal spinel, the affinity of Zinc ions towards the tetrahedral sites is more. Consequently, as the content of Zinc in the samples increases the amount of Zinc ions present on the A site also increases correspondingly. As a result the average bond length at a tetrahedral site (R_A) increases linearly with the content of Zinc in the sample. The variation of R_B with the Zn content is some what reverse. It can be seen that the R_B values decrease as the content of Zinc increases. This can be qualitatively explained on

the basis of formation of iono-covalent bonds at the B site. Since all the Zinc that is added occupies A sites the presence of magnesium ions and ferric ions at the B site results into an iono-covalent character of bonding at this site. Such a bonding has been explained by Dunitz and Orgel (16).

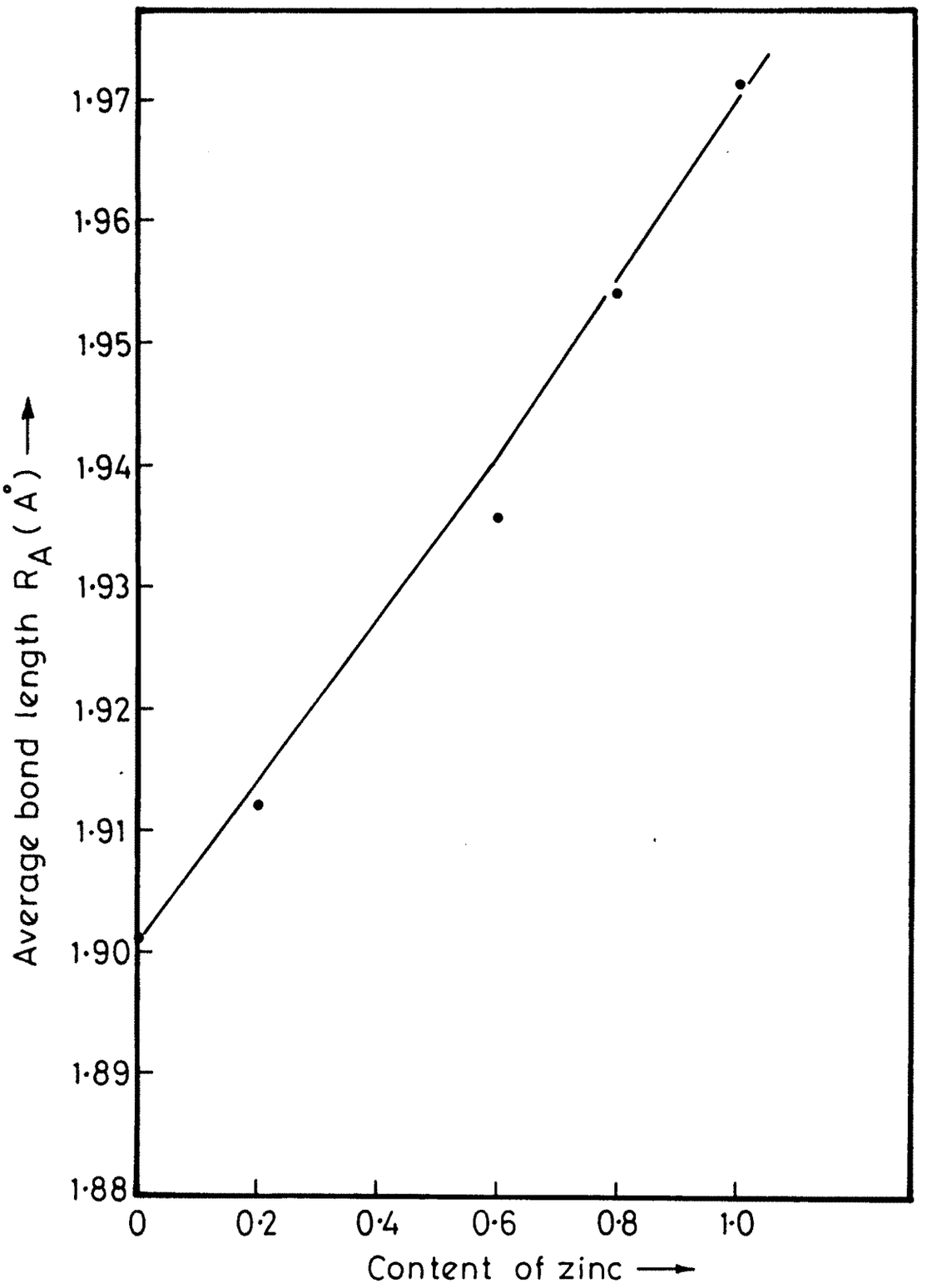
1·97
1·96
1·95
1·94
1·93
1·92
1·91
1·90
1·89
1·88
Average bond length R_A (Å)
0
0·2
0·4
0·6
0·8
1·0
Content of zinc

Fig.—2.9

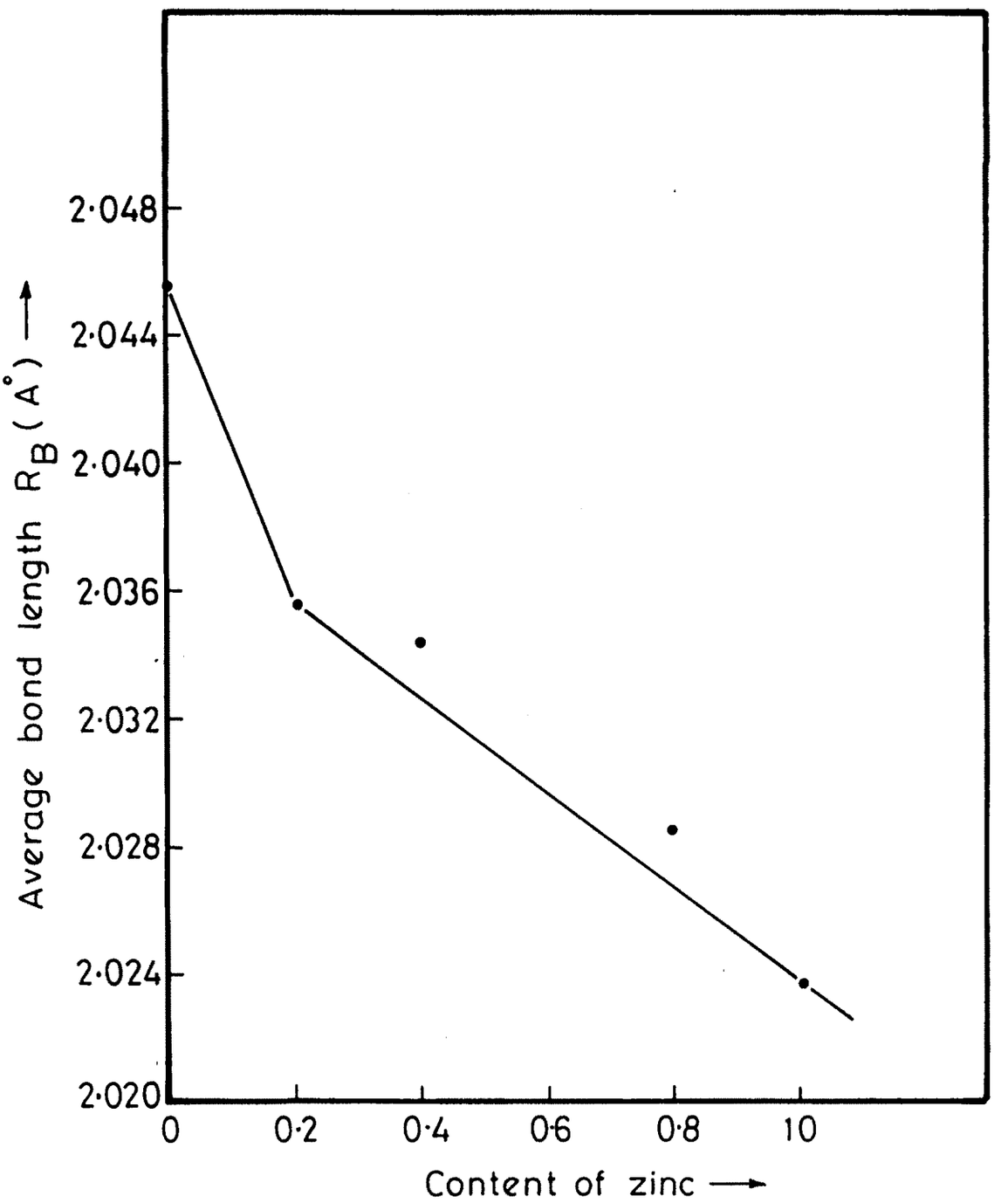
2·048
2·044
2·040
2·036
2·032
2·028
2·024
2·020
Average bond length R_B (Å) ⟶
0
0·2
0·4
0·6
0·8
1·0
Content of zinc ⟶

Fig.—2.10

TABLE- 2.9

AVERAGE BOND LENGTHS FOR $Mg_xZn_{(1-x)}Fe_2O_4$ FERRITE SINTERED AT 1100° C

CHEMICAL FORMULA	AVERAGE BOND LENGTH R_A	AVERAGE BOND LENGTH R_B
$MgFe_2O_4$	1.900	2.046
$Mg_{0.8}Zn_{0.2}Fe_2O_4$	1.916	2.039
$Mg_{0.6}Zn_{0.4}Fe_2O_4$	-	2.037
$Mg_{0.4}Zn_{0.6}Fe_2O_4$	1.945	-
$Mg_{0.2}Zn_{0.8}Fe_2O_4$	1.950	2.032
$ZnFe_2O_4$	1.980	2.029

REFERENCES

1. Economos G., J. Amer. Ceram . Soc.38,241(1955).

2. Robbins H., in "Ferrites", Proceeding of Third International Conference on Ferrites, Kyoto,Japan (29 Sept., 2 Oct. 1980)

3. Wolf W.P., Rodrigues G.P.,J.Appl.Phys.29,105(1958).

4. Sato T., IEEE Trans MAG, 6,795(1970)

5. Sato, T., Juroda C.,Saito M., in "Ferrites", Proc. Int.Conf. on Ferrites, Kyoto, Japan P.72 (1970)

6. Bragg W.L., Nature (London) 95, 561 (1915).

7. Debye, P., and Sherrer, P., Physic 17,277 (1916).

8. Hull A.N., Phy. Rev. 9, 84, 564 (1916) and ibid 10, 661 (1917).

9. Sawant S.R. and Patil R.N. "Magnetization and structural studies on cu ferrite", Indian Journal of Pure and Applied Physics, Vol.21, pp. 145-147,(1983)

10. Joshi G.K.,Deshapande S.A., Khot A.Y., and Sawant S.R., "Lattice parameter cation distribution and bond length studies of $Zn_xMg_{(1-x)}Fe_2O_4$ system".

Preprint.

11. Corliss L.M., Hestings J.M., Brockman F.G., Phys Rev, p. 90, 1013(1953).

12. Bacon G.E. and Roberts F.F., Acta. Cryst. P. 6,57 (1953).

13. Hestings J.M. and Corliss L.M., Rev.Mod. Phys, p. 25,114(1953)

14. Lotgering F.K., Phil. Res. Rept., p.11, 190, 337(1956).

16. Standley,K.J. "Oxides Magnetic Materials", Clarendon Press, Oxford, P.28 (1972)

17. Dunitz J.D. and Orgel L.E., J. Phys. Chem. Solids (GB) 3, 318 (1957).